Measurement of the second-order coherence of pseudothermal light

Tom A. Kuusela[a)]
Department of Physics and Astronomy, University of Turku, 20014 Turku, Finland

(Received 1 March 2016; accepted 18 January 2017)

We describe photon statistics experiments using pseudothermal light that can be performed in an undergraduate physics laboratory. We examine the light properties in terms of a second-order coherence function, as determined either by measuring the light intensity as a function of time or via coincidence analysis of a pair of photon detectors. We determine the coherence time and intensity distribution of the pseudothermal light source that exhibits either Gaussian or non-Gaussian statistics as a function of their optical parameters, and then compare the results with theoretical predictions. The simple photodiode method can be used for the qualitative analysis of the coherence time, but more accurate measurements are achieved using the coincidence method.
[http://dx.doi.org/10.1119/1.4975212]

I. INTRODUCTION

The introduction of second-order temporal coherence $g^{(2)}(\tau)$ is the most important development step in the history of quantum optics.[1–4] Experiments with beamsplitters performed by Brown and Twiss and their observation of photon bunching in light emitted by a chaotic source stimulated the birth of modern quantum optics.[5,6] Moreover, $g^{(2)}$ provides a nice tool for characterizing and classifying the basic types of light: thermal, coherent laser, and single photon light. Because $g^{(2)}$ can be explained within the framework of classical electromagnetism, it also gives undergraduate students a natural approach to understanding some basic features of light.

Measurement of $g^{(2)}(\tau)$ for natural thermal light is challenging because of the very short coherence time of these sources, typically only a few femtoseconds. This measurement problem was solved by Martienssen and Spiller when they introduced the construction of a *pseudothermal* source in which a laser beam is focused on rotating ground glass, which acts as a scatterer.[7] This concept was used later to experimentally demonstrate the photon bunching phenomenon.[8,9] This kind of pseudothermal source has since been used in numerous fundamental studies of photoelectron statistics and even as student laboratory experiments.[10] However, minimal attention has been paid to the optical parameters that significantly affect the time scale of the second-order coherence and the features of the intensity distribution.[11,12]

Here, we describe simple low-cost experiments using a pseudothermal source based on a rotating ground disk that can be adapted for use in an undergraduate laboratory. Since the coherence time of this source is long, light intensity fluctuations can be directly measured with a photodiode and the second-order coherence can be determined numerically as the autocorrelation function of the intensity time series. This can be regarded as the most classical method of measuring $g^{(2)}(\tau)$. We also describe $g^{(2)}$ measurements obtained by sending a beam of light onto a beamsplitter and measuring the correlations between the reflected and transmitted output intensities. This approach is more natural with respect to quantum optics. We show how the coherence time and intensity distribution depends on the features of the ground glass, the laser, and the focusing optics. We also compare the experimental results of these two measurement approaches with theoretical predictions. These photon statistics experiments can serve as a complementary approach to recently developed photon counting experiments designed for use in student laboratories.[13,14]

II. SECOND-ORDER TEMPORAL COHERENCE

If the intensity $I(t)$ of light is measured at one point in space and the statistical properties of the intensity do not change in time, the *second-order temporal coherence* is given by

$$g^{(2)}(\tau) = \frac{\langle I(t)I(t+\tau)\rangle}{\langle I(t)\rangle^2}. \tag{1}$$

The brackets normally indicate a time average but they can be replaced by the ensemble average for stationary light fields. If the fluctuations of the intensity are measured as a time series, $g^{(2)}(\tau)$ can be determined as the normalized *autocorrelation function* of the intensity and it can be proved that for classical fields $1 \le g^{(2)}(0)$ and $g^{(2)}(\tau) \le g^{(2)}(0)$.[15]

The actual functional form of $g^{(2)}$ for *thermal* sources depends on the details of the process by which the total electric field is created. If the oscillating electric field consists of a single frequency component but the phase of the oscillation changes randomly and abruptly in time, we have

$$g^{(2)}(\tau) = 1 + e^{-|\tau|/\tau_c}, \tag{2}$$

where τ_c is the coherence time.[15] This simple model corresponds to collisionally broadened thermal light, where more or less isolated atoms radiate. The corresponding frequency spectrum of the intensity time series has a *Lorentzian* shape. Another perspective is to recognize that the electric field has many different frequency components with a Gaussian distribution, and each component has a randomly distributed but constant phase. In this case, the atoms are close enough to interact with each other, giving[15]

$$g^{(2)}(\tau) = 1 + e^{-(\tau/\tau_c)^2}. \tag{3}$$

This kind of thermal light is called *Gaussian* because of the shape of the frequency spectrum, and it corresponds to Doppler broadened light.[16] The value $g^{(2)}(0)$ is commonly

used to classify different types of light.[15] In both Eqs. (2) and (3), $g^{(2)}(\tau)$ has a maximum value of 2 when $\tau = 0$, as it should be in the case of thermal light.[17]

The second order coherence function can be also determined using a beamsplitter and subsequent coincidence analysis of a pair of photon detectors.[18] In this case, Eq. (1) is replaced with

$$g^{(2)}(\tau) = \frac{\langle I_T(t) I_R(t+\tau)\rangle}{\langle I_I(t)\rangle^2}, \tag{4}$$

where I_T is the intensity of the transmitted beam, I_R is the intensity of the reflected beam, and I_I is the intensity of the input beam. According to the semiclassical theory of photoelectric detection, the conversion of the electromagnetic field into photoelectrons is a random process. The probability of obtaining a single photocount within a short time window Δt is proportional to the average intensity measured by the detector.[18,19] Probabilities can be approximated by the measured (over the total counting time ΔT) counts N_T, N_R, and N_{TR} to obtain[20]

$$g^{(2)}(\tau) = \frac{N_{TR}}{N_T N_R}\left(\frac{\Delta T}{\Delta t}\right). \tag{5}$$

III. EXPERIMENTAL SETUP

Figure 1 shows a schematic diagram of our experimental setup. The main component is the rotating ground glass that we use as a source of pseudothermal light. The rotation speed is fixed at 6.75 Hz, which corresponds to a period of 148 ms. The laser source (a collimator pen) has an output power of 1 mW, a wavelength of $\lambda = 637$ nm, a beam diameter of 4 mm at the focusing lens, and a total divergence of $\theta_{\text{div}} = 0.3$ mrad. The laser beam passes through a focusing lens (of focal length $f = 100$ mm, except in one measurement series where lenses with focal lengths of 35, 50, 70, and 13 mm were also used) onto the ground glass wheel (diameter of 25 mm, 1500-grit polished; see later comments), 7 mm from the rotation axis. The distance F from the waist of the laser beam to the ground glass was varied between 0 and 20 mm.

After the baffle, the light is either measured with the photodiode (with an iris 1.0 mm in diameter) and recorded by a digital oscilloscope (sampling frequency 100 kHz) or collected with the multimode optical fiber (core diameter 62.5 μm) without any focusing optics and directed to the beamsplitter for coincidence analysis. The laser light is attenuated with a neutral density filter. The single and coincidence counts are recorded using a time-to-digital converter; the width of the coincidence window is 10 ns.

IV. PROPERTIES OF SPECKLE PATTERNS

When the laser beam shines on the ground glass, the roughness of the surface acts as a large set of scattering centers, which produce approximately spherical waves. Since these centers are randomly distributed, they produce complex interference patterns, or *speckles*, in the far field. If the number of surface details is high in the area of the laser spot, the spatial distribution of the field amplitude is Gaussian, which is a manifestation of the central limit theorem.[21]

If the laser spot is tightly focused, the speckles on the screen are large but if the spot itself is large, the patterns are small.[7] Further, the speckles seem to move if the ground glass rotates, and while this might seem quite natural, the real situation is fairly complex.[11,12] If the distance F from the waist to the ground glass is decreased, the speckle pattern moves faster. Further, if the laser waist is in front of the surface ($F > 0$; see Fig. 1) the speckles move in the same direction as the scattering surface. If the waist is on the surface ($F = 0$), the speckles do not move at all but simply evolve *in situ*. And finally, if the laser waist is behind the surface ($F < 0$), the speckles move in the direction opposite to that of the scatterer. The explanation for all of these phenomena is the fact that the moving speckles can be observed only when the laser light has a nonzero curvature on the ground glass. Laser light, which is often modeled as a Gaussian or TEM_{00} beam, has zero curvature only at the waist (and at infinity).[22]

Detailed calculations have shown that with a Gaussian laser beam, in the limit of very many scatterers, $g^{(2)}(\tau)$ has the form of Eq. (3) and the coherence time is given by[11,12]

$$\tau_c = \frac{W_0}{v\left[(1+F/L)^2 + y^2\right]^{1/2}}, \tag{6}$$

where $W_0 = \frac{1}{2} f \theta_{\text{div}}$ is the radius of the waist, v is the velocity of the surface of the ground glass at the center of the laser spot (the circumferential path length multiplied by the rotation frequency), and L is the distance from the glass to the detector. The parameter $y = kW_0^2/2L$, with $k = 2\pi/\lambda$ the wavenumber of the laser light, determines whether the

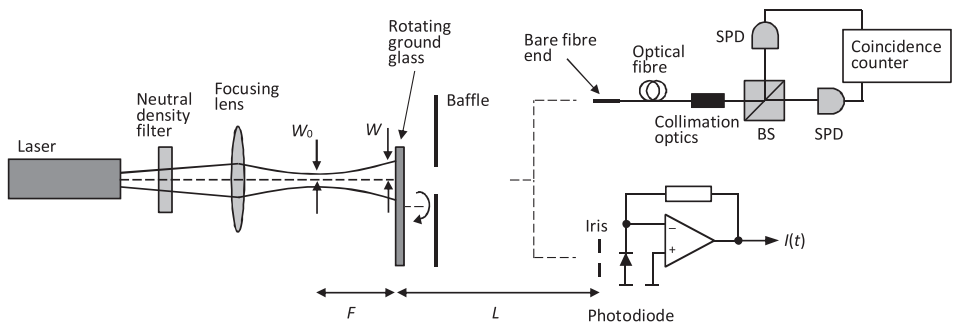

Fig. 1. Experimental setup: W_0 is the radius of the waist of the laser beam, W is the radius of the laser spot on the ground glass, F is the distance from the waist to the ground glass, and L is the distance to either the photodiode or the end of collecting fiber from the ground glass. The single photon detectors (SPDs) are connected to the output ports of the beamsplitter (BS), and single and coincidence counts from the detectors are analyzed in the counter module.

detectors are in the near field ($y \gg 1$) or far field ($y \ll 1$). In our system, we always measured intensities in the far field. We note that τ_c is *not* the time taken for a new independent set of scatterers to enter the laser spot. Actually, when F/L is small, τ_c only weakly depends on F and hence on the size W of the region of the scatterers illuminated by the laser beam. If the divergence of the beam is not known, the radius of the beam waist can be roughly estimated as $W_0 = f\lambda/D$ where D is the diameter of the beam at the aperture. The divergence can also be determined by measuring the fraction of the beam power transmitted by various circular apertures at various distances.

V. RESULTS

Figure 2 shows the intensity of the pseudothermal light measured with the photodiode as a function of time, and this intensity varies in what appears to be a random manner. Strictly speaking, the intensity is not random but periodic; after rotation of the ground glass the intensity repeats its course. However, in our experiments the period of the intensity could not be determined, either from the time series or from its power spectrum.

We calculated the second-order coherence $g^{(2)}(\tau)$ based on the photodiode measurements, as stated in Eq. (1). We calculated the intensity autocorrelation of the digitized data using home-made software,[23] but these calculations can be done by almost any software capable of numerical calculations, even spreadsheet programs. We note that the calculation of the autocorrelation is highly sensitive to any offsets in the input data, either due to background light, a photodiode dark current, or an input offset voltage of the amplifier. If there is any offset, it should be removed prior to autocorrelation analysis. When the waist of the laser beam is on the ground glass, the characteristic Gaussian shape of $g^{(2)}(\tau)$ is observed, as shown in Fig. 3. However, the maximum value of $g^{(2)}(0) = 1.74 \pm 0.02$ (Ref. 24) is well below the theoretical value of 2.

In the case of a waist distance of 10 or 20 mm, the autocorrelation is almost constant. The obvious reason for this is the fact that the speckle patterns are so small that the detector has averaged out the smallest spatial details. By using a smaller iris diameter in front of the photodiode, we could restore the correct shape of $g^{(2)}(\tau)$ but the lower signal level and poorer signal-to-noise ratio can prevent accurate measurements, unless the output power of the laser source is increased. In the case of non-rotating ground glass, the intensity is practically constant on these time scales (there are minor slow variations in the laser intensity) and thus $g^{(2)}(\tau) = 1$ (data not shown). We can conclude that if the diameter of the iris or the active area of the photodiode itself is small enough, qualitative measurements of $g^{(2)}(\tau)$ can be performed at the very least.

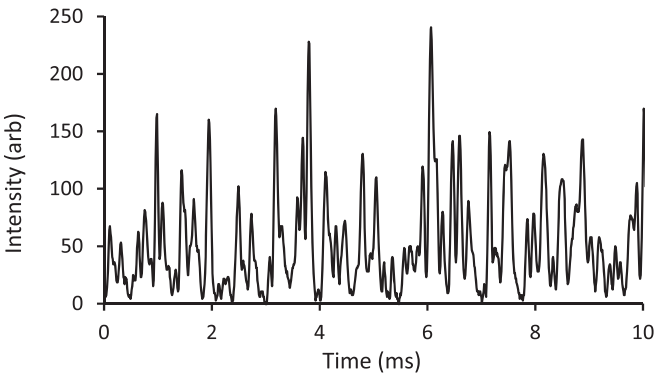

Fig. 2. Intensity of the pseudothermal light measured with the *photodiode*. In this case, the waist distance F from the ground glass was zero.

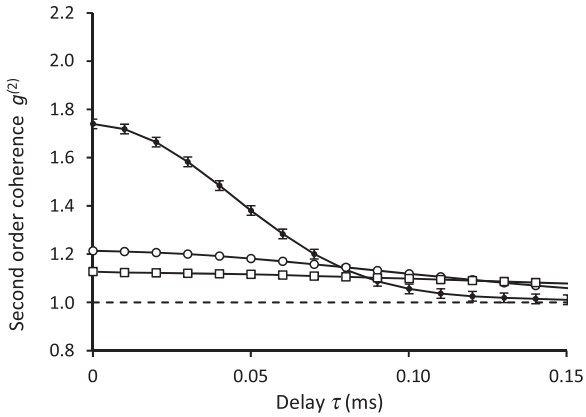

Fig. 3. Second-order coherence as a function of the delay time measured with the photodiode. The waist distances F from the ground glass were 0 mm (solid dots), 10 mm (open dots), and 20 mm (open rectangles). For reference, the value $g^{(2)} = 1$ is shown as a dashed line. The data points are connected by lines for clarity. Error bars represent one standard deviation.

Figure 4(a) shows the second-order coherence at different waist distances as a function of the delay time, as measured with a beamsplitter and a coincidence analysis of the outputs, according to Eq. (5). The maximum values of $g^{(2)}$ are closer to 2, which is a clear indication of less spatial averaging due to the very small aperture of the optical fiber. When the ground glass is not rotating, we get $g^{(2)}(\tau) \approx 1$ as expected for stable laser light. The shape of $g^{(2)}(\tau)$ is very close to Gaussian, as demonstrated in Fig. 4(b). When comparing our experimental data ($F = 0$) with the Gaussian function of Eq. (3) using the theoretical prediction $\tau_c = 0.051$ ms from Eq. (6), we can see that the deviations are almost within the range of measurements errors. The maximum value of $g^{(2)} = 1.96 \pm 0.03$ when $F = 0$, but it drops as the waist distance is increased. This behavior indicates that even when using optical fiber, spatial averaging can be significant.

By fitting the theoretical prediction of Eq. (3) to the results shown in Fig. 4(a), we determined the delay time τ_c as a function of the waist distance F. The delay time decreases slowly when this distance increases (see Fig. 5), as expected from Eq. (6), since the ratio F/L is quite small. As seen in the figure, the experimental results are close to the theoretical prediction. For example, at zero distance, experimentally we have $\tau_c = 0.052 \pm 0.003$ ms while the theoretical prediction was $\tau_c = 0.051$ ms. We note that the most inaccurate parameter in the measurement system is the position of the laser spot on the ground glass, which directly affects the velocity v in Eq. (6).

In order to further validate Eq. (6), we also varied the radius of the waist W_0. We performed this experiment using five lenses with different focal lengths and based our experiments on the beamsplitter method. In all cases, we adjusted the waist of the beam to the surface of the ground glass so that $F = 0$. As can be seen in Fig. 6, the dependence of the delay time on the focal length is quite linear and close to the theoretical prediction; deviations are within the error bars.

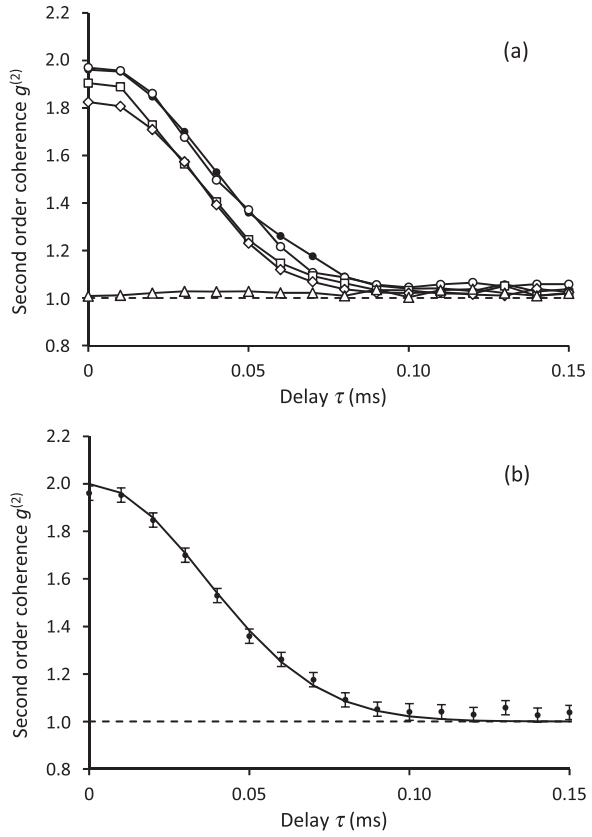

Fig. 4. (a) Second-order coherence as a function of the delay time determined by the beamsplitter and coincidence analysis. The waist distances F from the ground glass were 0 mm (solid dots), 5 mm (open dots), 15 mm (open rectangles), and 20 mm (open diamonds). For reference, the results for non-rotating ground glass are also shown (open triangles). The data points are connected by lines for clarity. (b) The $F = 0$ data (solid dots) from (a) and the Gaussian function [solid line, Eq. (3)] that uses the theoretical prediction from Eq. (6) for τ_c. Error bars represent one standard deviation.

These results demonstrate that the coherence time can be varied by nearly an order of magnitude simply by changing the focusing lens.

The large number of scatterers is the key assumption for all the previous theoretical considerations. Under this condition, the distribution of the field amplitudes is Gaussian and thus so is the distribution of the intensities. Because the mean size of the scatterers of a 1500-grit polished ground glass is well below 5 μm,[25] and the diameter of the laser spot

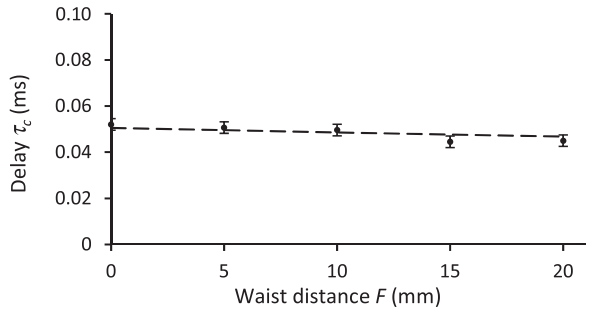

Fig. 5. Delay time τ_c as a function of the distance of the laser beam waist F. The theoretical prediction based on Eq. (6) is shown as a dashed line. The focal length of the focusing lens was 100 mm. Error bars represent one standard deviation.

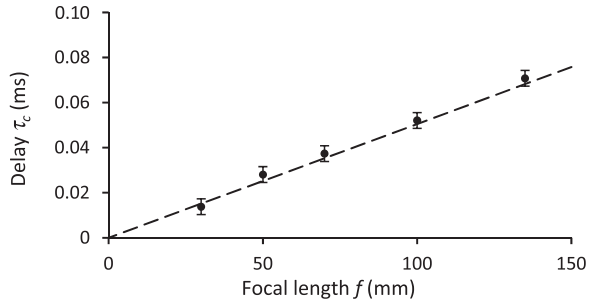

Fig. 6. Delay time τ_c as a function of the focal length f of the focusing lens (35, 50, 70, 100, and 135 mm). The distance F of the waist from the surface of the ground glass was 0 mm in each case. The theoretical prediction based on Eq. (6) is shown as a dashed line. Error bars represent one standard deviation.

was 30 μm ($F = 0$), at any given time there are approximately 150 scatterers illuminated by the laser beam. Such a high number of scatterers guarantees the expectation of a Gaussian distribution. From time series data collected with the photodiode, we could compute the intensity distribution, as shown in Fig. 7. As the data (solid dots) are well-fit by a straight line on the logarithmic scale, the Gaussian character of the distribution is clear.

For our final experiment, we replaced the original 1500-grit ground glass with 120-grit polished ground glass, which corresponds to less than 10 scatterers in the area of the laser spot. In this case, the intensity had very sharp peaks and long periods of zero values, as shown in Fig. 8, and the intensity distribution is no longer Gaussian (see Fig. 7, open dots). Figure 9 shows the corresponding second-order coherence determined by the beamsplitter method. It no longer has a Gaussian shape, and the maximum value is 3.2, significantly higher than the value 2 for the Gaussian case. Further, the coherence seems to be a combination of a Gaussian [Eq. (3)] in the small time delays and Lorentzian [Eq. (2)] in the longer time delays. Since the form of the second order coherence is related to the details of the spatial distribution of the

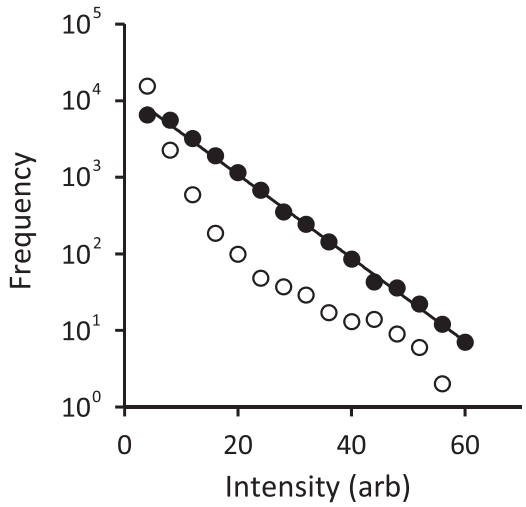

Fig. 7. Distribution of intensity for Gaussian (1500-grit ground glass, solid dots) and non-Gaussian (120-grit ground glass, open dots) light. The laser beam waist was located on the ground glass ($F = 0$). The Gaussian distribution fits well on a straight line in the logarithmic scale (correlation coefficient 0.99). Error bars representing one standard deviation are smaller than the markers.

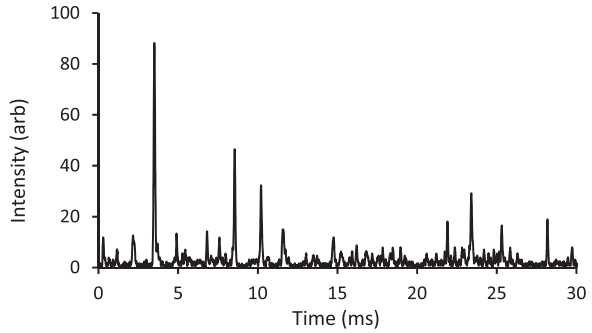

Fig. 8. Intensity of the pseudothermal light measured using the photodiode with ground glass of 120-grit. The waist distance from the ground glass was 0 mm.

scatterers when the number of scatterers is low, these observations can give some information regarding the surface properties of the ground glass.[11] In general, the calculation of the distribution of the scatters from the measured $g^{(2)}(\tau)$ is a challenging inverse problem. However, we can assume that the Lorentzian characteristic of $g^{(2)}$ is due to the well-localized and larger scratches of the surface, which produce abrupt changes in the intensity, and Gaussian character is due to the many small-scale spatial details of those structures. Direct microscopical inspections of the surface gave us some hints of this kind of texture. Finally, we note that we could recover the pure Gaussian shape of $g^{(2)}$ if we increased the size of the beam waist by changing the focal length of the lens or increasing the distance of the waist from the ground glass.

VI. CONCLUSION

Pseudothermal light demonstrates various aspects of many physical phenomena and therefore its experimental analysis with respect to second-order coherence can be useful in undergraduate and graduate courses in classical and quantum optics and atomic physics. Using the most minimal setup, the fluctuations in light intensity can be measured and captured using only a photodiode and a digital oscilloscope, from which it is then possible to determine the coherence as a function of the delay time, at least qualitatively, depending on the optical setup. Because of the almost unavoidable spatial averaging of the photodiode, this method has some limitations. However, by directly recording the light intensity, it is possible to determine the intensity distribution and draw some conclusions regarding the number of scatterers. Using an optical fiber to collect light, a beamsplitter and single photon detectors (equipment quite commonly available nowadays in student laboratories), more accurate measurements of second-order coherence can be performed and real comparisons made with theoretical predictions. Our experimental results indicate that accurate results can be achieved for various sets of optical parameters.

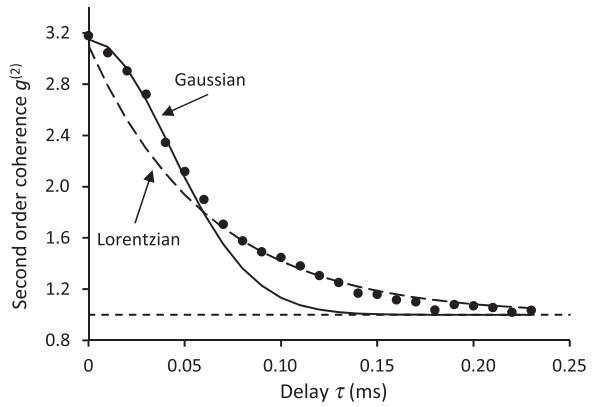

Fig. 9. Second-order coherence of non-Gaussian pseudothermal light determined by the beamsplitter method ($F = 0$). Data have been fitted with both Gaussian (small time delays) and Lorentzian (large time delays) forms of coherence.

[a]Electronic mail: tom.kuusela@utu.fi

[1]P. Grangier, G. Roger, and A. Aspect, "Experimental evidence for a photon anticorrelation effect on a beam splitter: A new light on single-photon interference," Europhys. Lett. **1**, 173–179 (1986).
[2]C. W. Chou, S. V. Polyakov, A. Kuzmich, and H. J. Kimble, "Single-photon generation from stored excitation in an atomic ensemble," Phys. Rev. Lett. **92**, 213601 (2004).
[3]A. B. U'Ren, C. Silberhorn, J. L. Ball, K. Banaszek, and I. A. Walmsley, "Characterization of the nonclassical nature of conditionally prepared single photons," Phys. Rev. A **72**, 021802 (2005).
[4]C. Santori, S. Gotzinger, Y. Yamamoto, S. Kako, K. Hoshino, and Y. Arakawa, "Photon correlation studies of single GaN quantum dots," Appl. Phys. Lett. **87**, 051916 (2005).
[5]R. Hanbury Brown and R. Q. Twiss, "Correlation between photons in two coherent beams of light," Nature (London) **177**, 27–29 (1956).
[6]R. Q. Twiss, A. G. Little, and R. Hanbury Brown, "Correlation between photons in two coherent beams of light, detected by a coincidence counting technique," Nature (London) **180**, 324–326 (1957).
[7]W. Martienssen and E. Spiller, "Coherence and fluctuations in light beams," Am. J. Phys. **32**, 919–926 (1964).
[8]F. T. Arecchi, "Measurement of the statistical distribution of Gaussian and laser sources," Phys. Rev. Lett. **15**, 912–916 (1965).
[9]F. T. Arecchi, E. Gatti, and A. Sona, "Time distribution of photons from coherent and Gaussian sources," Phys. Lett. **20**, 27–29 (1966).
[10]L. Basano and P. Ottonello, "New correlator-photon counter to illustrate the fundamentals of light statistics," Am. J. Phys. **50**, 996–1000 (1982).
[11]E. Jakeman, "The effect of wavefront on the coherence properties of laser light scattered by target centres in uniform motion," J. Phys. A **8**, L23–L28 (1975).
[12]P. N. Pusey, "Photon correlation study of laser speckle produced by a moving rough surface," J. Phys. D **9**, 1399–1409 (1976).
[13]P. Koczyk, P. Wiewior, and C. Radzewicz, "Photon counting statistics—Undergraduate experiments," Am. J. Phys. **64**, 240–245 (1996).
[14]M. L. Martinez Ricci, J. Mazzaferri, A. V. Bargas, and O. E. Martinez, "Photon counting statistics using a digital oscilloscope," Am. J. Phys. **75**, 707–712 (2007).
[15]R. Loudon, *The Quantum Theory of Light* (Oxford U.P., New York, 2000).
[16]It is important not to confuse the Gaussian distribution of the electric field amplitude (or intensity) with the frequency distribution. Thermal light with a Lorentzian frequency spectrum is called Gaussian-Lorentzian and light with a Gaussian frequency spectrum is called Gaussian-Gaussian light. However, it is also possible to have chaotic or random light, which has a non-Gaussian amplitude distribution.
[17]For single photon light $g^{(2)}(0) = 0$ and for coherent light $g^{(2)}(0) = 1$, see Ref. 15.
[18]J. J. Thorn, M. S. Neel, V. W. Donato, G. S. Bergreen, R. E. Davies, and M. Beck, "Observing the quantum behavior of light in the undergraduate laboratory," Am. J. Phys. **72**, 1210–1219 (2004).
[19]M. Beck, "Comparing measurements of $g^{(2)}$ performed with different coincidence detection techniques," J. Opt. Soc. Am. B **24**, 2972–2978 (2007).
[20]L. Mandel and E. Wolf, *Optical Coherence and Quantum Optics* (Cambridge U.P., Cambridge, 1995).
[21]The "Central Limit Theorem" states that the sum of a large number of independent random variables (having more or less equal distribution) will be approximately normally distributed, regardless of the underlying distribution. See, for example, P. Billingsley, *Probability and Measure* (John Wiley & sons, New York, 1995).
[22]I. R. Kenyon, *The Light Fantastic: A Modern Introduction to Classical and Quantum Optics* (Oxford U.P., New York, 2011).

[23]See supplementary material at http://dx.doi.org/10.1119/1.4975212 for Software, in the form of a Windows executable program.
[24]Error estimates here and in all further analyses are based on one standard deviation calculated over 20 sets of measurements, not the standard error of the mean.
[25]The grit size comes from the number of standardized holes that fit within the standard dimensional sized screen used to characterize the particle dimensions of the polishing material. Unfortunately, this number varies from one manufacturer to another. Here, the size of the scatterers was estimated visually using a microscope.

Junkers-Type Calorimeter

This handsome piece of copper-work is listed in the 1940 Cenco catalogue at $14.00. It is specifically designed to measure the heating properties of gas. Gas for domestic use is fed at a measured rate to a burner placed under the body of the calorimeter. The hot air travels up through a number of flues running through the volume of water running past the heated copper inside, and the increase in the temperature of the water is monitored as a function of the amount of gas consumed. This instrument is in the Greenslade Collection. (Picture and Notes by Thomas B. Greenslade, Jr., Kenyon College)